



HAWC results on binary systems

Vardan Baghmanyant

Institute of Nuclear Physics, Krakow, Poland

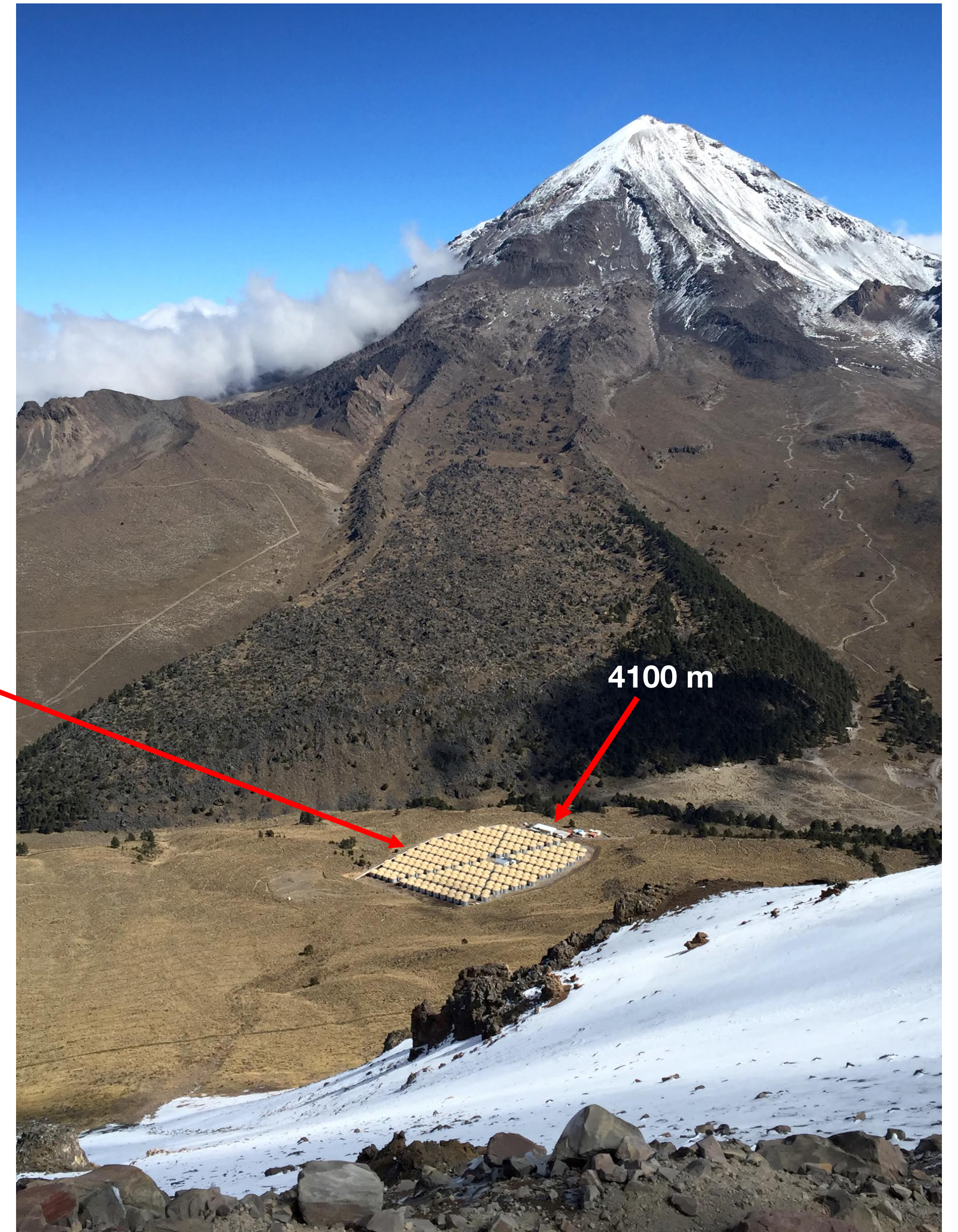
Outline

- The HAWC Observatory
- Binary candidates in HAWC FOV
- Multi TeV emission from the lobes of SS 433
- Recent studies of SS 433 with Fermi-LAT compared to HAWC results
- Conclusions and Outlook

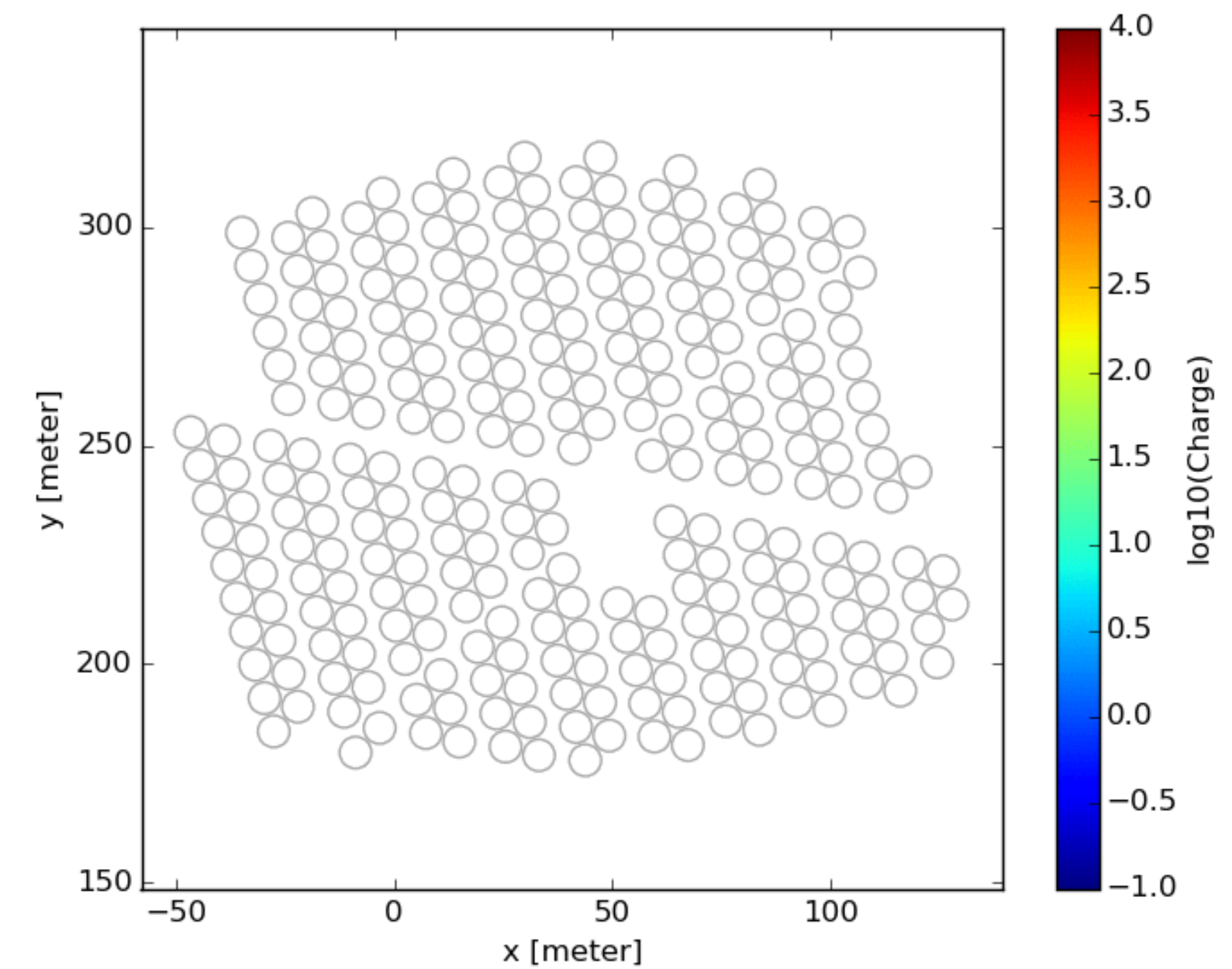
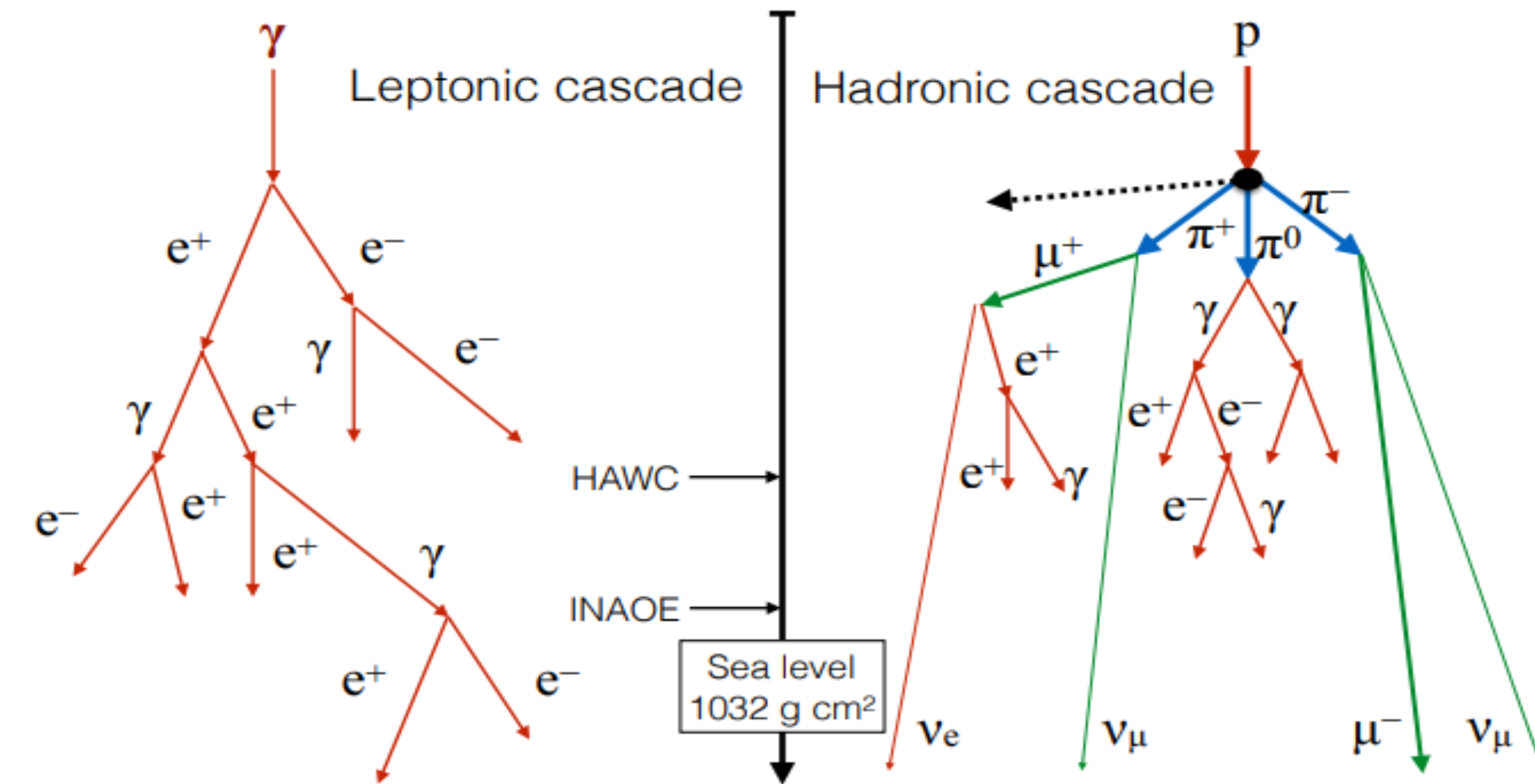
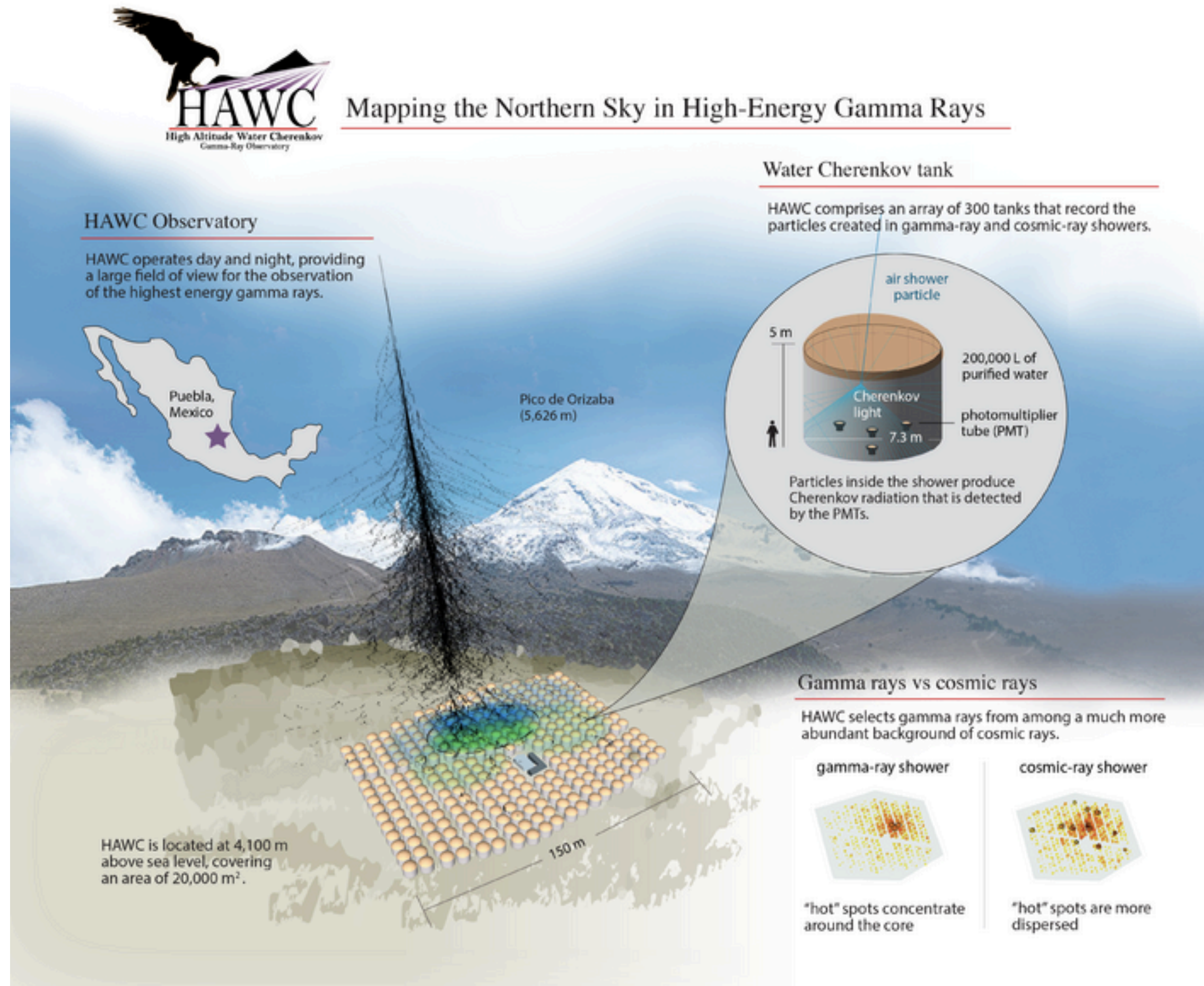
The HAWC observatory



Site: Sierra Negra, Mexico, 19°N, 4,100 m altitude.
Instantaneous FOV 2 sr. (15%) and daily 8sr (66%).
Duty cycle >90%.
300 WCDs covering 22,000 m² area.



The structure and principles of operation

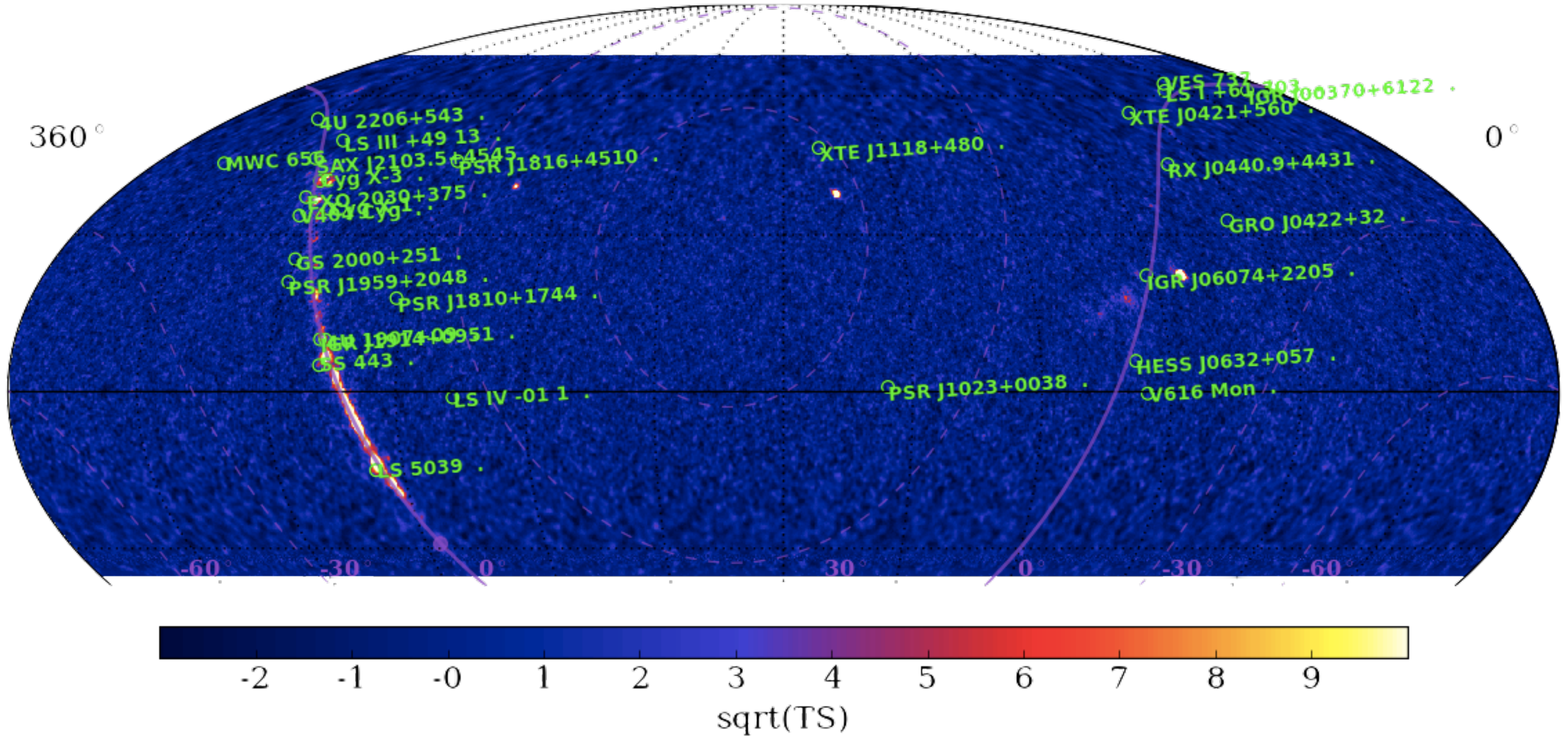


- The interactions of cosmic ray or photon with a nucleus from the air produces a shower of secondary particles.
- Cherenkov light produced by secondary particles, passed through the water in the tanks, is detected with PMTs.
- Event reconstruction
 1. Obtain the shower core position
 2. Fit the shower direction
 3. Estimate the shower energy by computing event size, PMT charge, etc.

Scientific objectives

- Primary cosmic-ray studies between 1 TeV and 1 PeV
- Studies of Galactic (pulsars, cosmic ray anisotropy, **binaries**) and extragalactic γ -ray sources
- Monitoring of TeV γ -ray transients and hard-spectrum sources
- Multi-wavelength studies with Fermi, Swift and IACTs telescopes
- Multi-messenger following ups on triggers from Neutrino telescopes and GW observatories
- Search for dark matter sources

Binary candidates in HAWC 1017d map



28 XRBs with short orbital periods and 3 known γ -ray binaries (LS I +61 303, LS 5039 and HESS J0632+057).

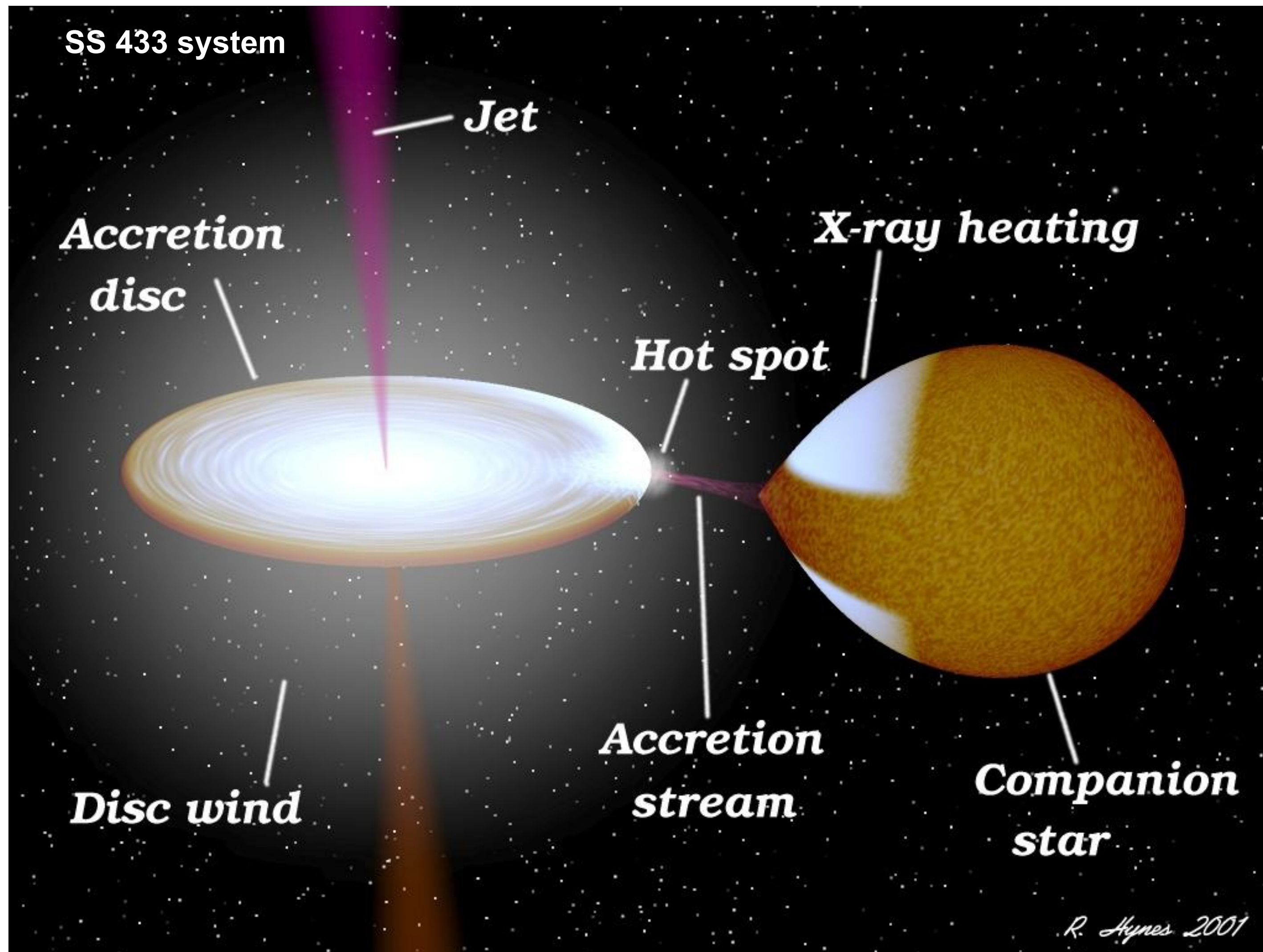
Short periods (<1 month), <10 kpc from Earth.

Table of binary candidates

Source	RA	Dec	Type	d [kpc]	τ [day]	TS	Signif. [post-trial]	Dif Flux @ 7 TeV [TeV ⁻¹ cm ⁻² s ⁻¹]
IGR J00370+6122	00:37	+61°21'	HMXB	3.4	15.67	3.6	-0.2 σ	$7.65 \cdot 10^{-15}$
V662 Cas	01:18	+65°17'	HMXB	6.5	11.60	0.0	0.0 σ	$4.13 \cdot 10^{-14}$
IGR J01363+6610	01:36	+66°11'	HMXB	2.0	-	1.8	-0.0 σ	$2.46 \cdot 10^{-14}$
IGR J01583+6713	01:58	+67°13'	XB	4.1	-	0.3	0.0 σ	$8.44 \cdot 10^{-14}$
VES 737	02:20	+63°01'	Bin	5.0	-	1.3	0.0 σ	$4.81 \cdot 10^{-14}$
LS I +61 303	02:40	+61°13'	HMXB	2.0	26.50	0.7	-0.0 σ	$1.40 \cdot 10^{-14}$
XTE J0421+560	04:19	+55°59'	HMXB	2.0	19.41	0.0	0.0 σ	$1.05 \cdot 10^{-14}$
GRO J0422+32	04:21	+32°54'	LMXB	2.0	0.21	1.3	0.0 σ	$3.33 \cdot 10^{-15}$
RX J0440.9+4431	04:40	+44°31'	HMXB	2.9	-	4.8	0.5 σ	$4.39^{+4.09}_{-3.43} \cdot 10^{-15}$
IGR J06074+2205	06:07	+22°05'	HMXB	4.5	-	0.3	-0.0 σ	$1.34 \cdot 10^{-15}$
V616 Mon	06:22	-00°20'	LMXB	1.1	0.33	0.1	-0.0 σ	$2.53 \cdot 10^{-15}$
HESS J0632+057	06:32	+05°48'	HMXB	1.6	315 ± 5	3.2	0.1 σ	$2.06^{+2.39}_{-1.94} \cdot 10^{-15}$
PSR J1023+0038	10:23	+00°53'	LMXB	1.3	-	5.3	0.7 σ	$3.13^{+2.83}_{-2.28} \cdot 10^{-15}$
XTE J1118+480	11:18	+48°02'	LMXB	1.7	0.17	4.9	0.6 σ	$5.57^{+5.20}_{-4.37} \cdot 10^{-15}$
LS IV -01 1	17:07	-01°05'	Star	0.3	-	0.1	-0.0 σ	$2.58 \cdot 10^{-15}$
PSR J1810+1744	18:10	+17°41'	MSP	2.0	-	1.2	0.0 σ	$2.89 \cdot 10^{-15}$
PSR J1816+4510	18:16	+45°10'	MSP	4.0	0.36	0.2	0.0 σ	$4.96 \cdot 10^{-15}$
LS 5039	18:26	-14°50'	HMXB	2.9	3.90	210.5	14.3 σ	$6.83^{+1.03}_{-1.01} \cdot 10^{-14}$
4U 1907+09	19:09	+09°49'	HMXB	4.0	8.37	13.4	2.7 σ	$4.22^{+2.42}_{-2.32} \cdot 10^{-15}$
SS 433	19:12	+04°59'	XB	5.5	13.10	19.2	3.6 σ	$5.21^{+2.48}_{-2.40} \cdot 10^{-15}$
IGR J1914+0951	19:14	+09°52'	HMXB	5.0	13.56	88.6	9.0 σ	$1.11^{+0.25}_{-0.25} \cdot 10^{-14}$
Cyg X-1	19:58	+35°12'	HMXB	2.2	5.60	5.0	0.6 σ	$2.81^{+2.58}_{-2.19} \cdot 10^{-15}$
PSR J1959+2048	19:59	+20°48'	Bin	2.5	-	2.6	0.0 σ	$3.43 \cdot 10^{-15}$
GS 2000+251	20:02	+25°14'	LMXB	2.7	0.35	0.0	0.0 σ	$2.07 \cdot 10^{-15}$
V404 Cyg	20:24	+33°52'	LMXB	2.4	6.47	1.3	0.0 σ	$3.61 \cdot 10^{-15}$
EXO 2030+375	20:32	+37°38'	HMXB	5.0	46.02	16.7	3.2 σ	$5.60^{+2.85}_{-2.82} \cdot 10^{-15}$
Cyg X-3	20:32	+40°57'	HMXB	7.0	0.20	98.9	9.6 σ	$1.73^{+0.37}_{-0.36} \cdot 10^{-14}$
LS III +49 13	20:56	+49°40'	BH	0.1	-	0.5	-0.0 σ	$4.13 \cdot 10^{-15}$
SAX J2103.5+4545	21:03	+45°45'	HMXB	6.5	12.68	0.1	0.0 σ	$5.26 \cdot 10^{-15}$
4U 2206+543	22:07	+54°31'	HMXB	2.6	9.57	2.2	-0.0 σ	$4.20 \cdot 10^{-15}$
MWC 656	22:42	+44°43'	HMXB	2.6	-	0.5	0.0 σ	$5.49 \cdot 10^{-15}$

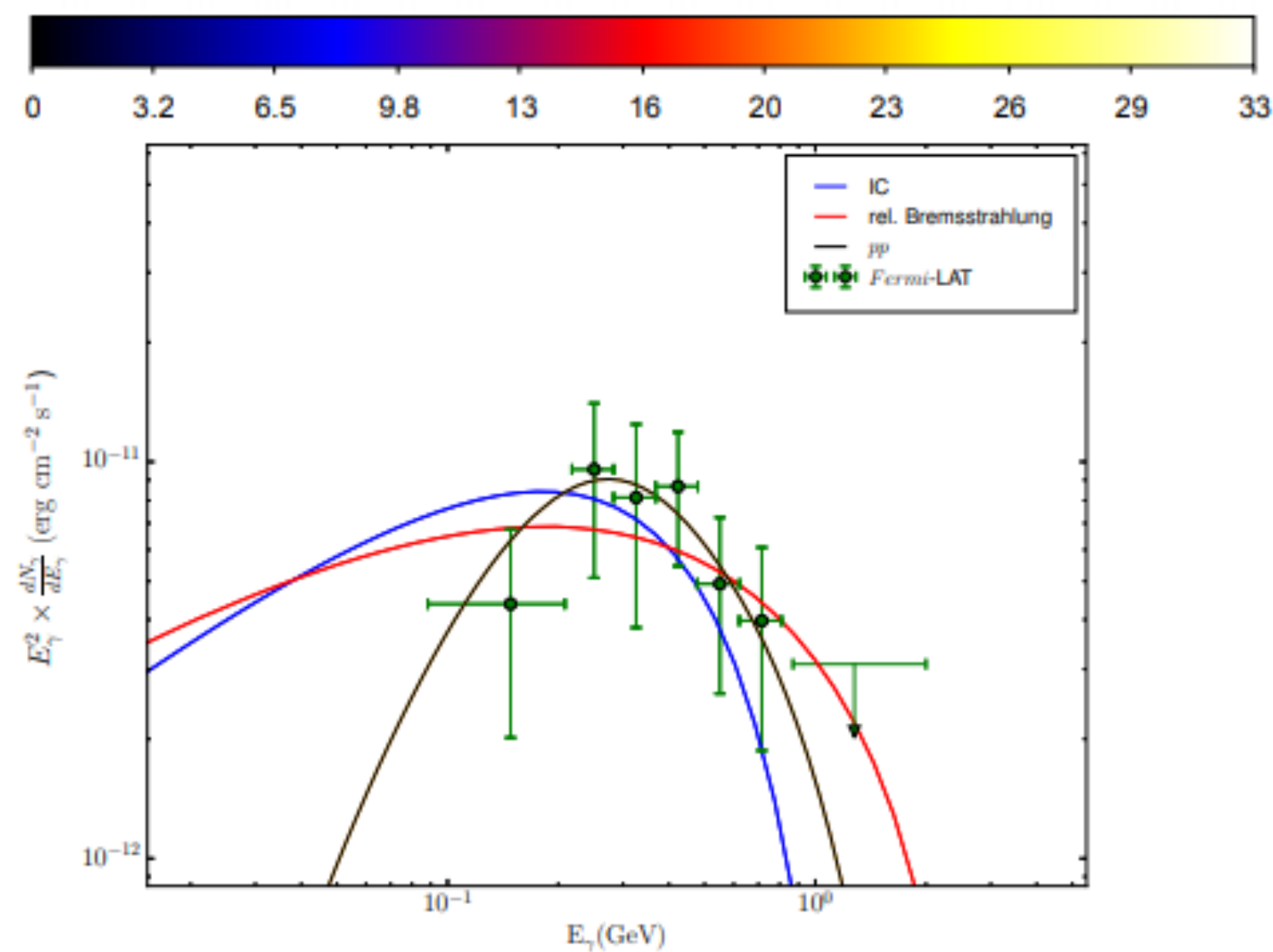
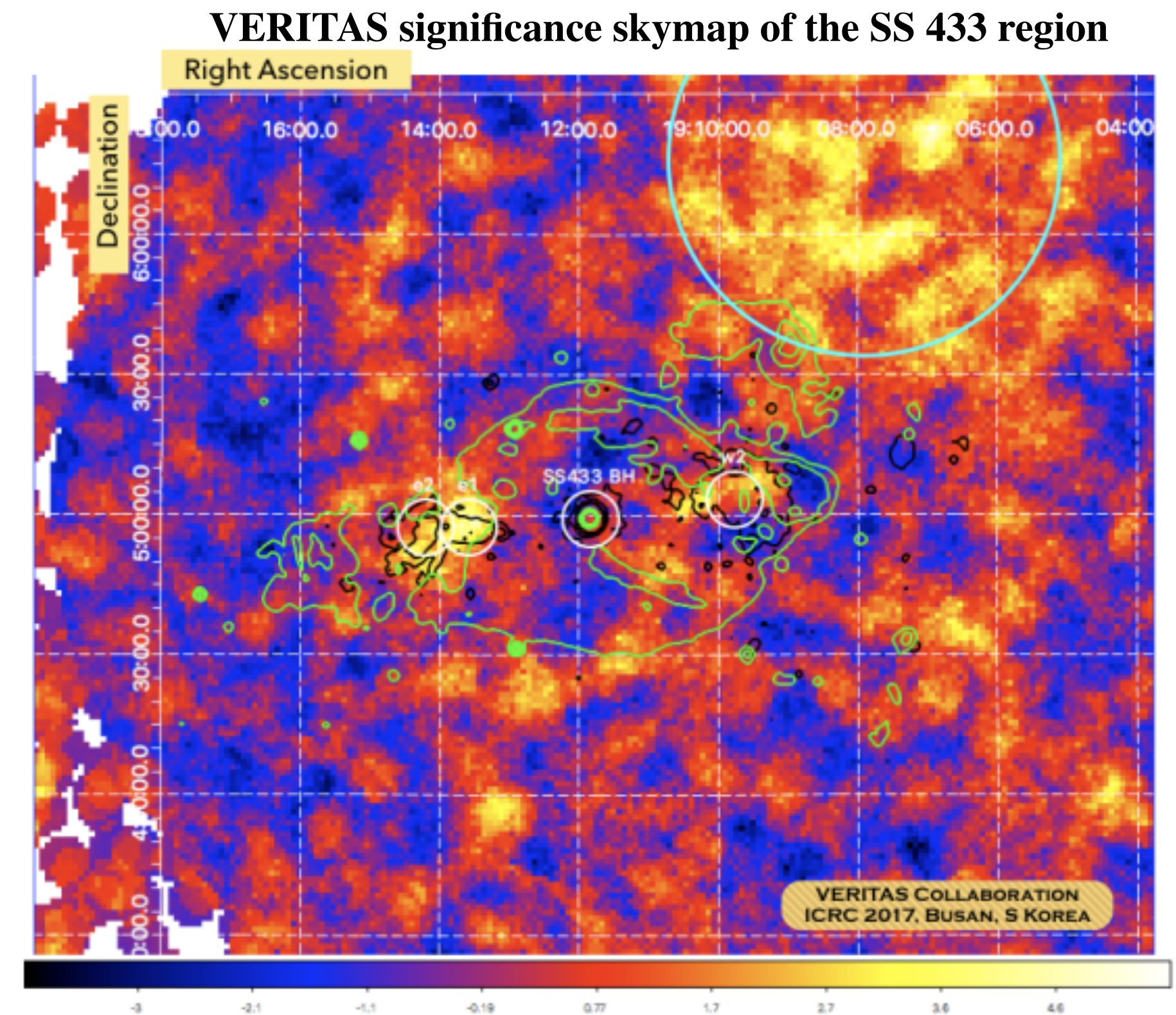
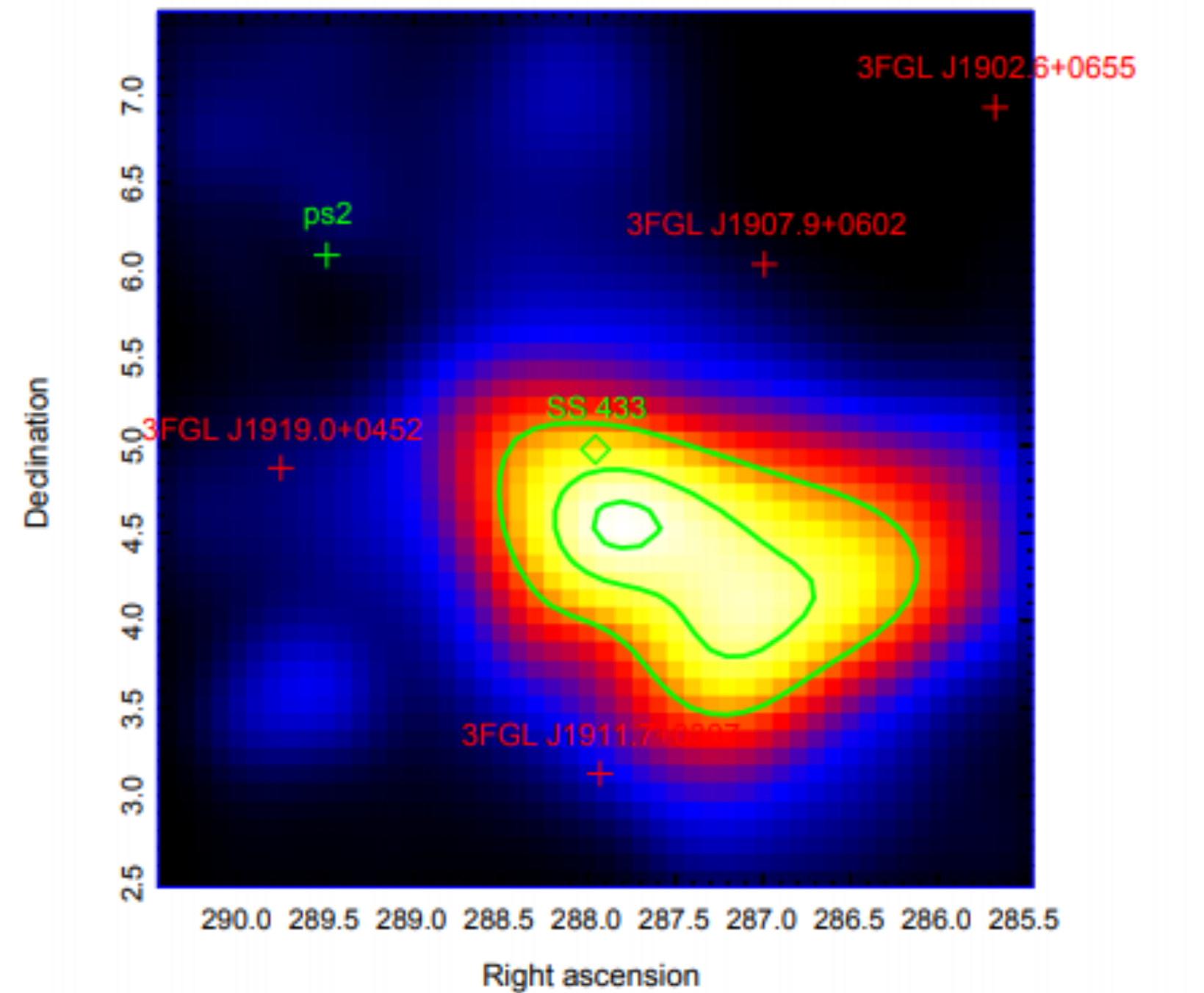
- Calculated TS after fitting a power law with a fixed index of -2.7 and Epiv at 7 TeV.
- Source confusion for objects in the Galactic Plane is an issue.
- Micro-quasar LS 5039 was isolated from confused region using multi-source fits, but HAWC does not yet have 5 σ observation.

Micro-quasars as sources of GeV/TeV gamma-rays: SS 433



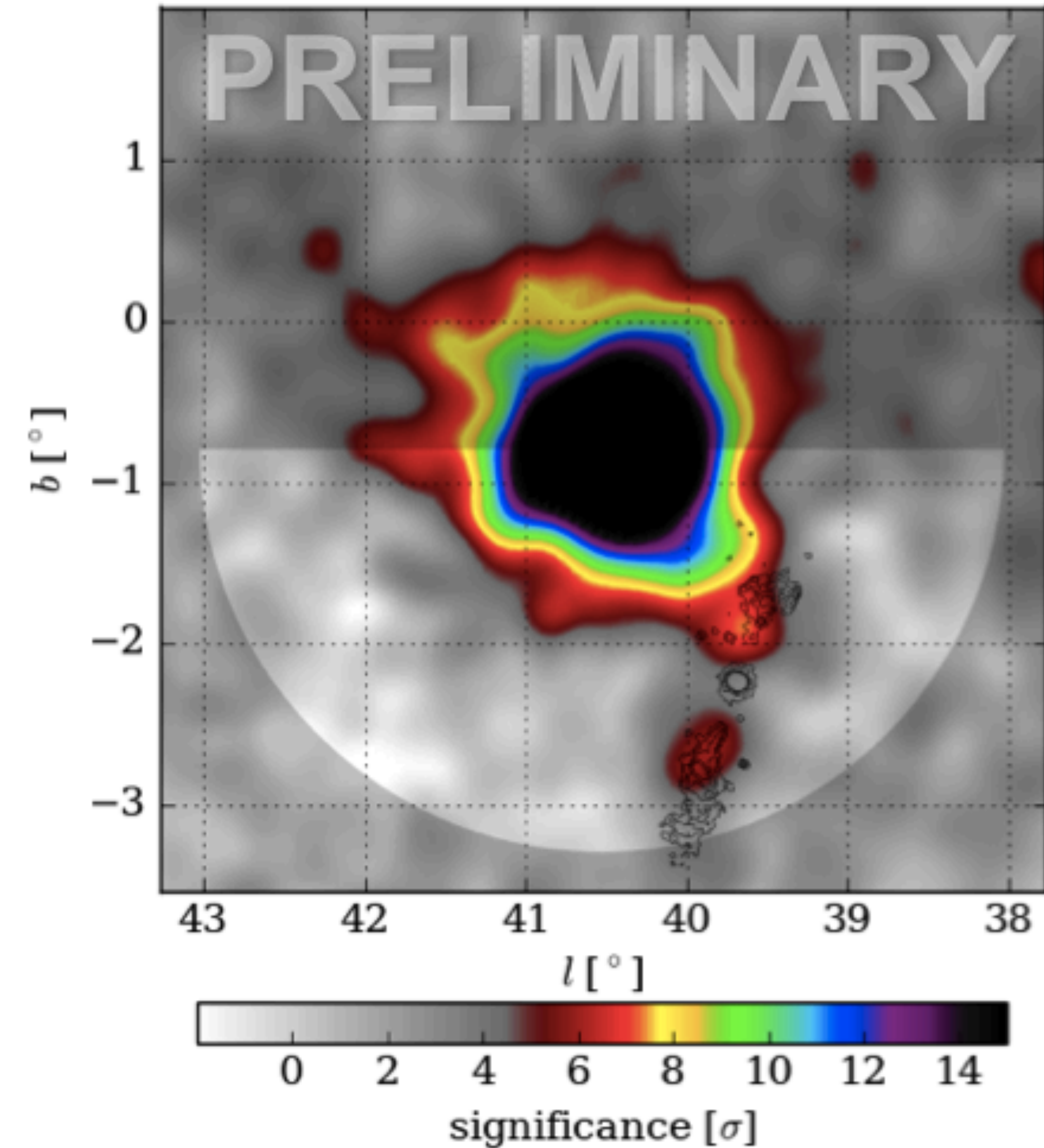
- Micro-quasars are binary stellar systems where the remnant of a star that has collapsed to form a dark and compact object is gravitationally linked to a star that still produces light, and around which it makes a closed orbital movement.
- SS 433 is a binary star consisting of an early type supergiant 30 solar masses star and a compact object (neutron star or black hole). Material from the normal star is falling toward the compact object, either as the result of a strong stellar wind, or through Roche lobe overflow.
- Two jets, the most powerful known in the Galaxy, extend perpendicular to the line of sight and terminate in W50 nebula producing western and eastern X-ray lobes.
- SS433 jet : 10^{39} - 10^{40} erg/s
- SS433 jet speed roughly $c/4$
- Particle acceleration is believed to occur at the lobes where strong radiation is expected to be emitted at GeV/TeV energies

SS 433 with Fermi and IACTs

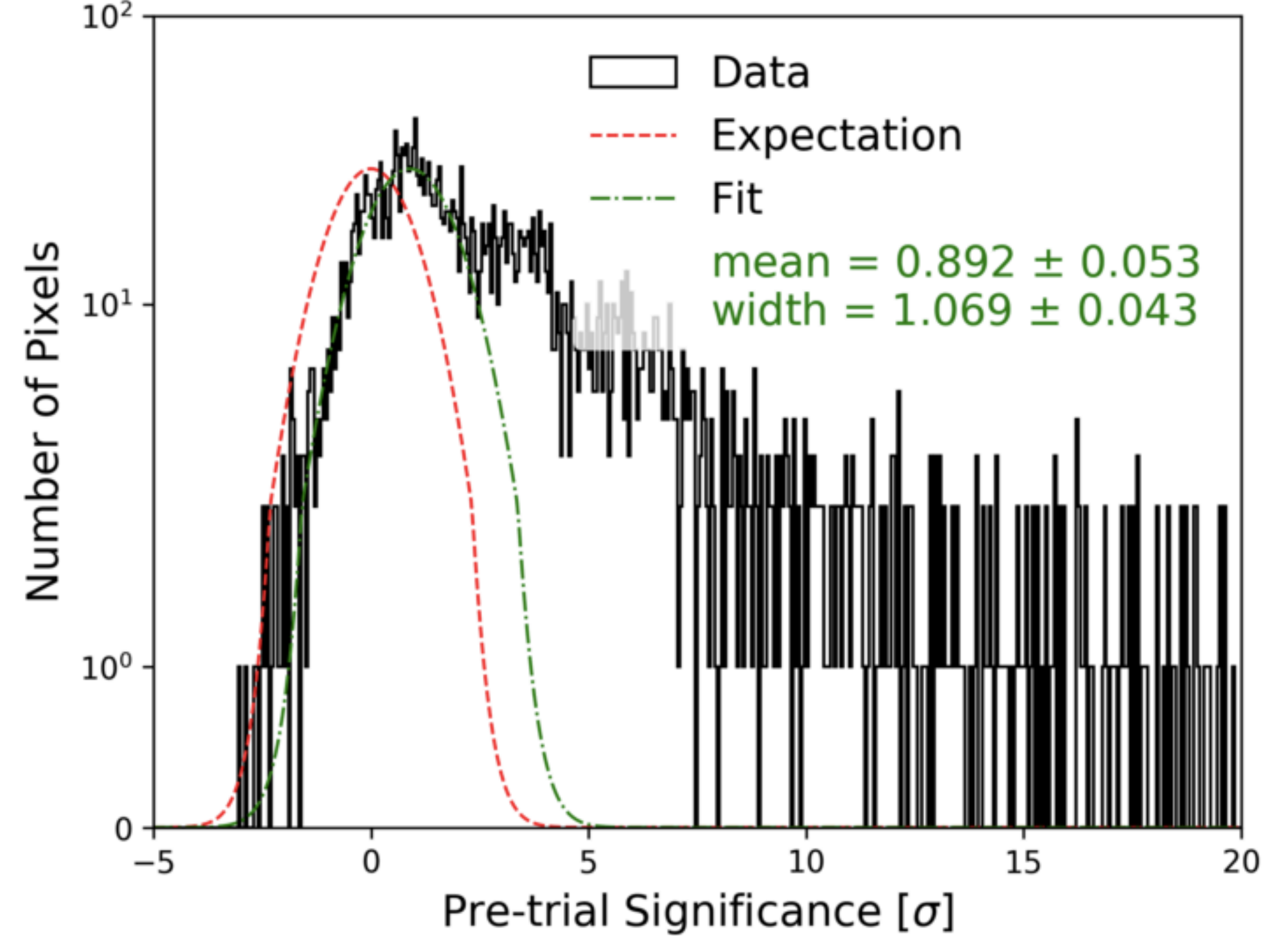


- Fermi-LAT analysis revealed a persistent gamma radiation between 250 MeV and 800 MeV, possibly due to proton-proton interaction close to SS433 (Bordas et al. 2015).
- The 70 hours (during 2009-2012) with VERITAS didn't detect significant emission from the location of the black hole or the jet termination regions (Payel Kar et al 2017).
- Combined HESS-MAGIC analysis produces only upper limits.

Region of SS 433 dominated by MGRO J1908+06

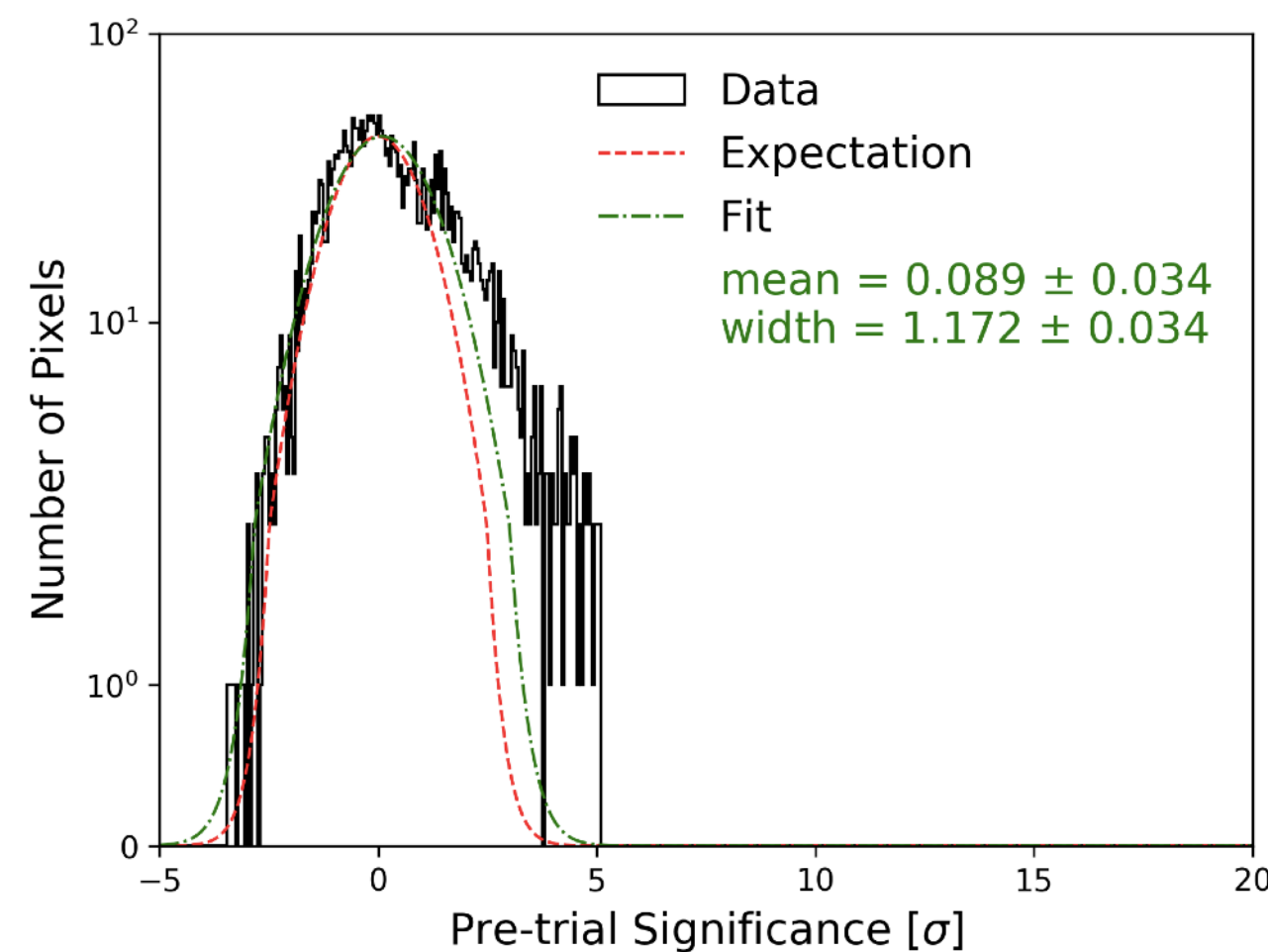
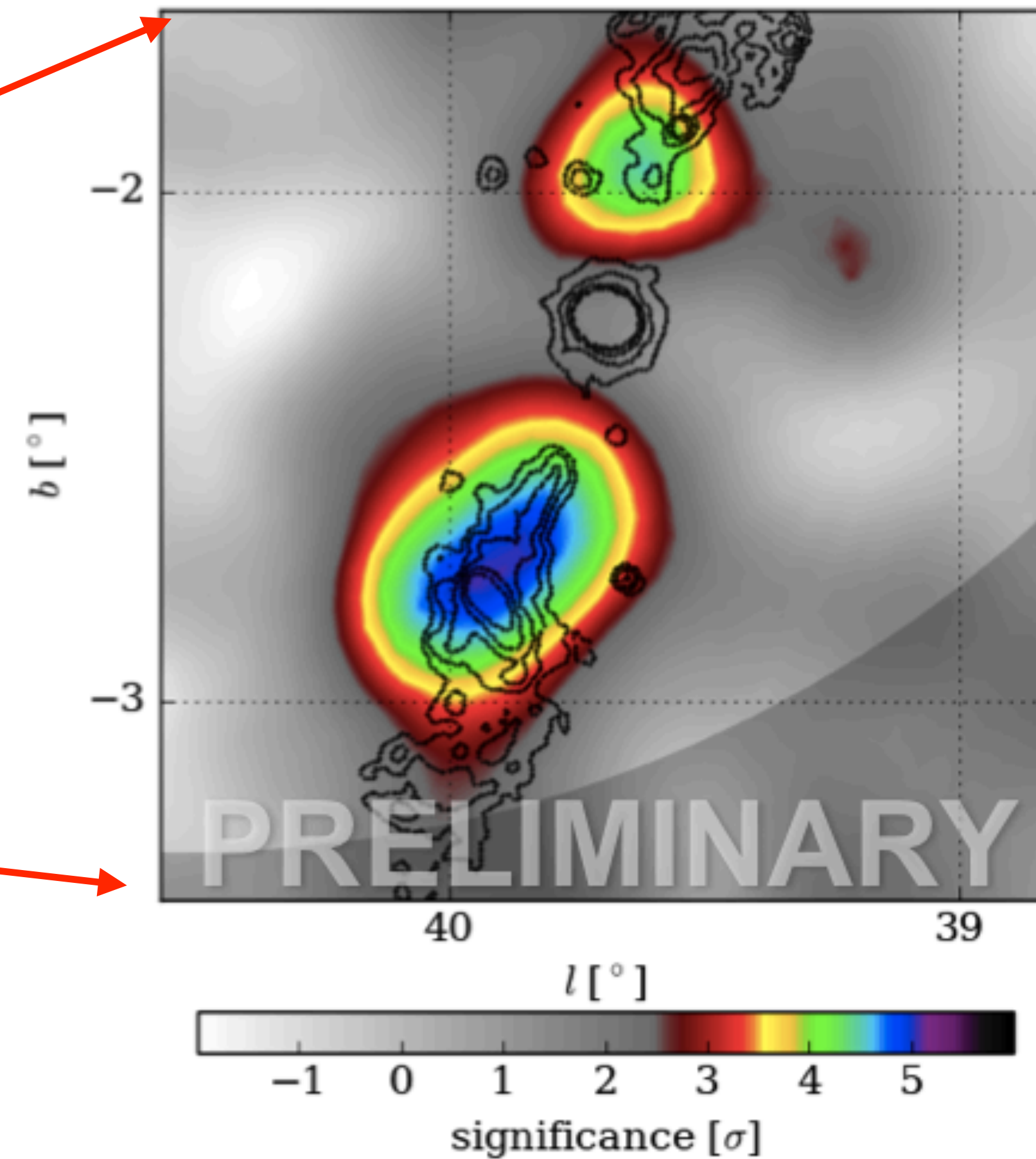
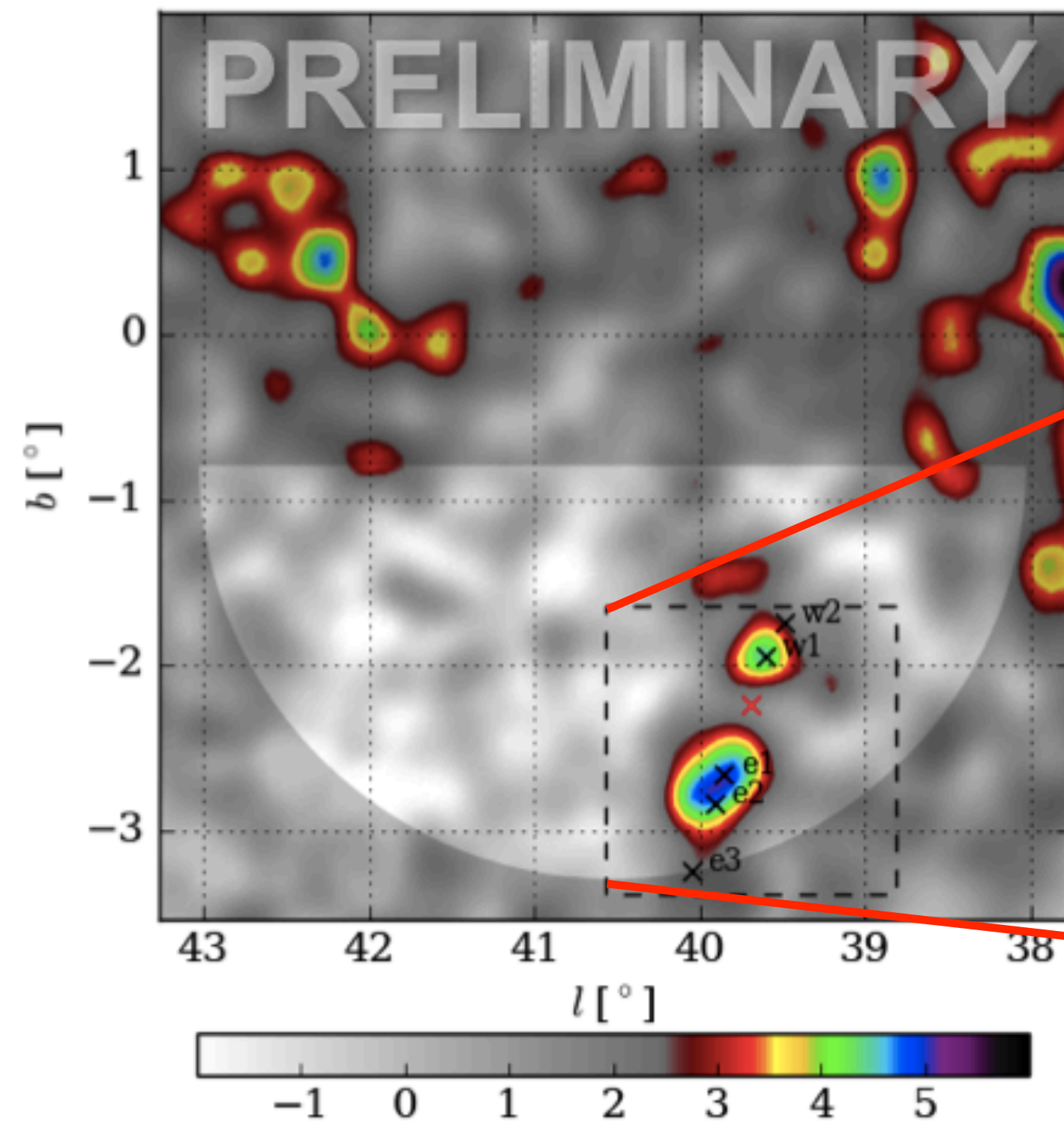


Distribution of pixel significance defined as deviations from the background expectation.



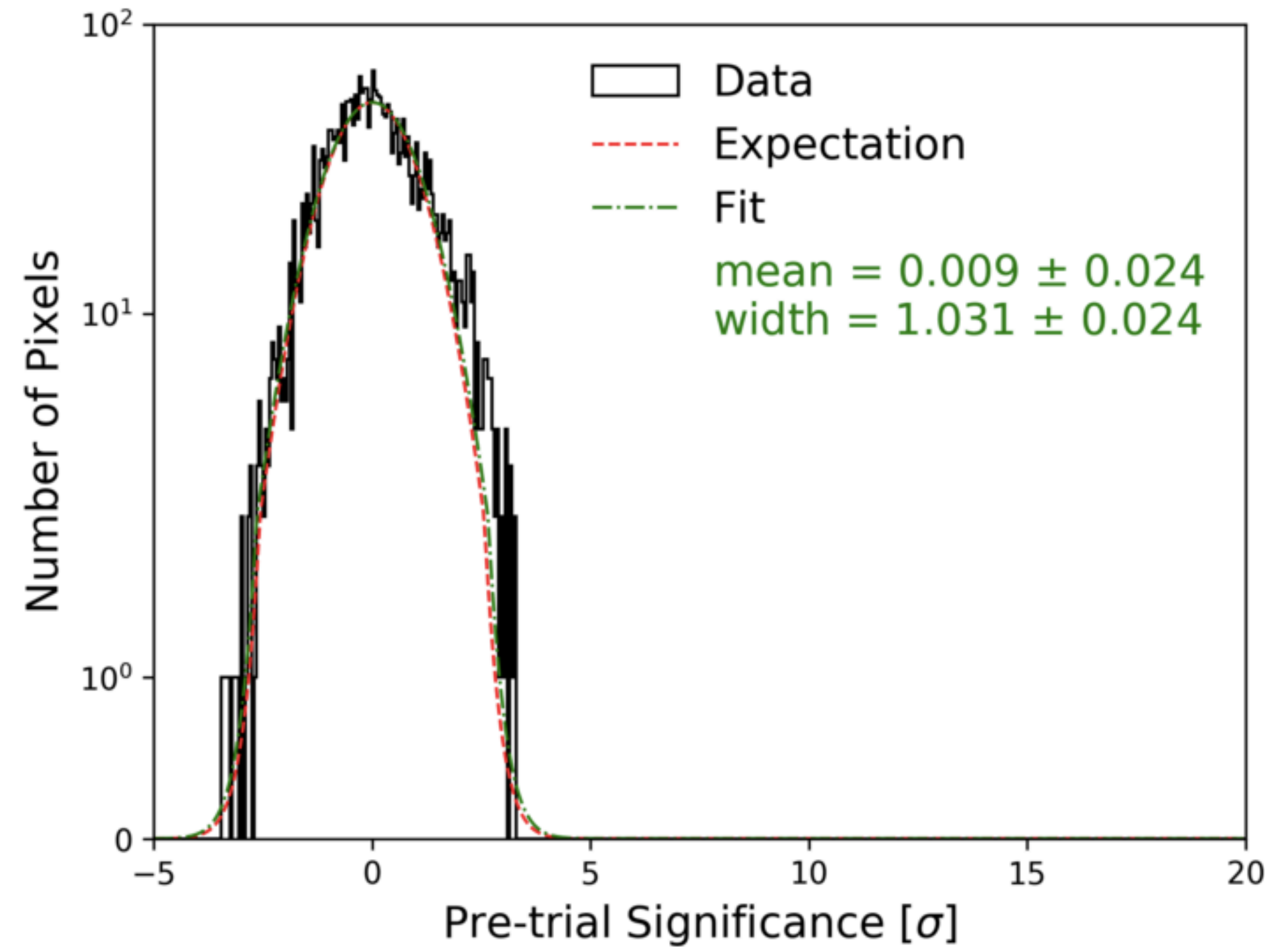
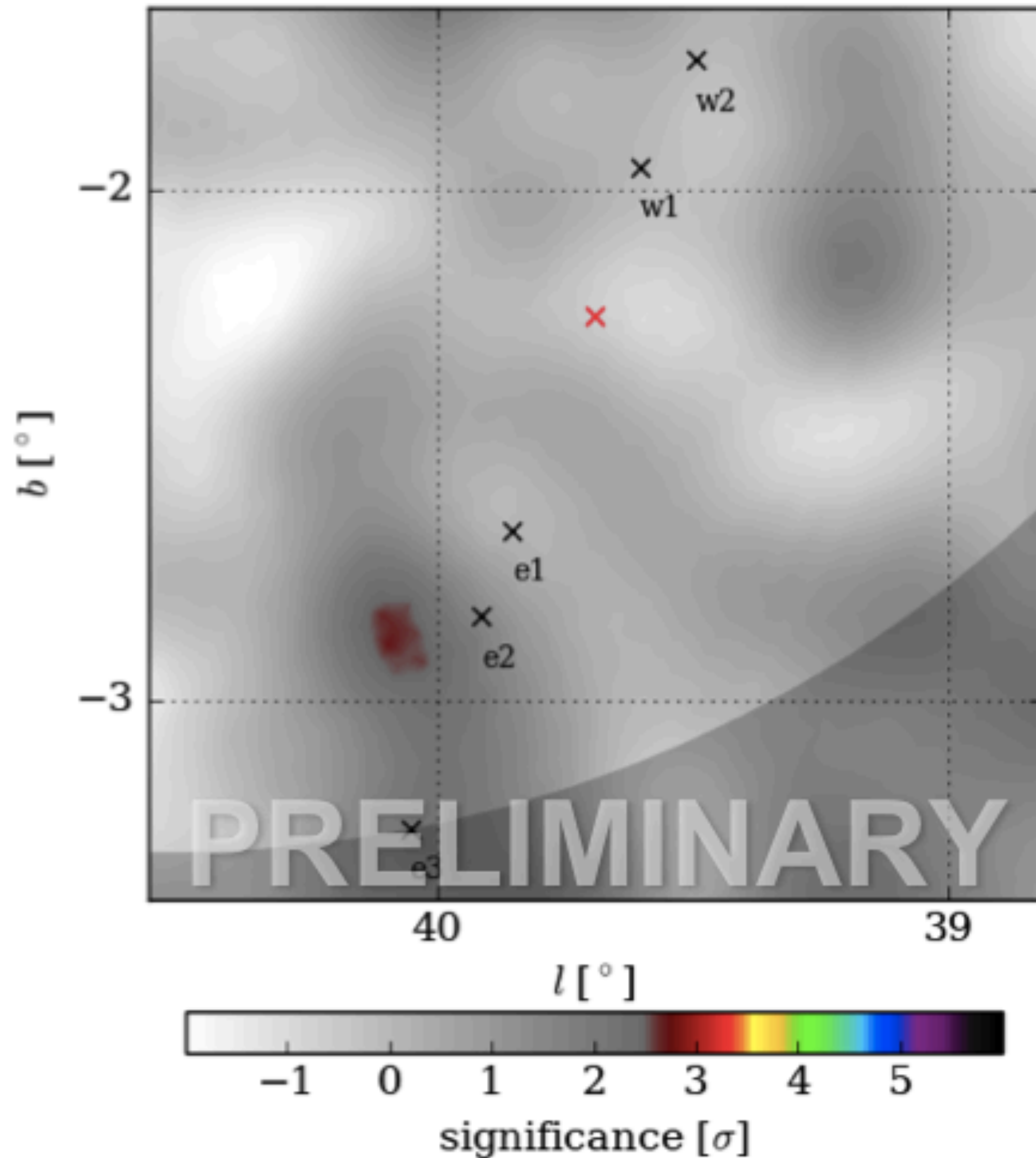
- Two SS 433 lobes and J1908 fitted simultaneously (normalisation, spectrum, size for MGRO J1908+06 and normalisation for each SS433 lobe)
- SS433 lobes spectral index assumed -2
- Semi-circular RoI to reduce GDE contamination

Region of SS 433 after subtracting MGRO J1908+06



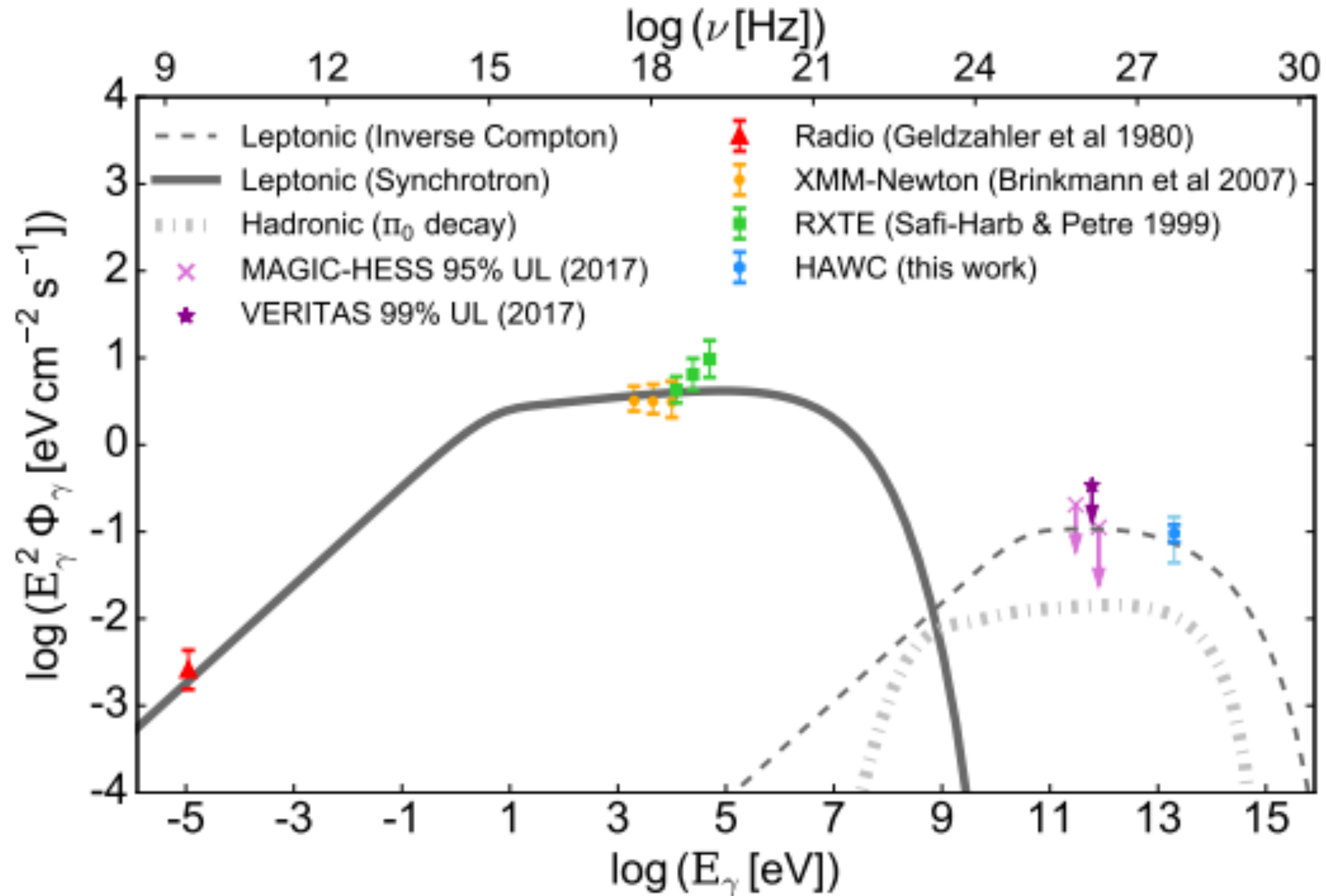
- PL of spectral index -2.0 has been assumed for both lobes.
- The pre-trial significance distribution shows improvement by removing J1908 but high significance tail still exists.

Residuals



- Residual map with J1908 + lobes fitted and subtracted
- The residual significance distribution is zero-mean Gaussian, consistent with background only distribution.
- The two lobes of SS433 are detected after a joint fit at a significance of 5.4σ being spatially coincident with the jet termination regions, where x-ray lobes are detected.

Multi-wavelength modeling (e1)



- Leptonic: radio + X-ray photons are produced via synchrotron emission in a magnetic field (16 microGauss) and TeV γ rays are produced via IC scattering of the same electron population with total kinetic energy equal to $\sim 0.5\%$ of the jet power.

Hadronic only model is disfavoured

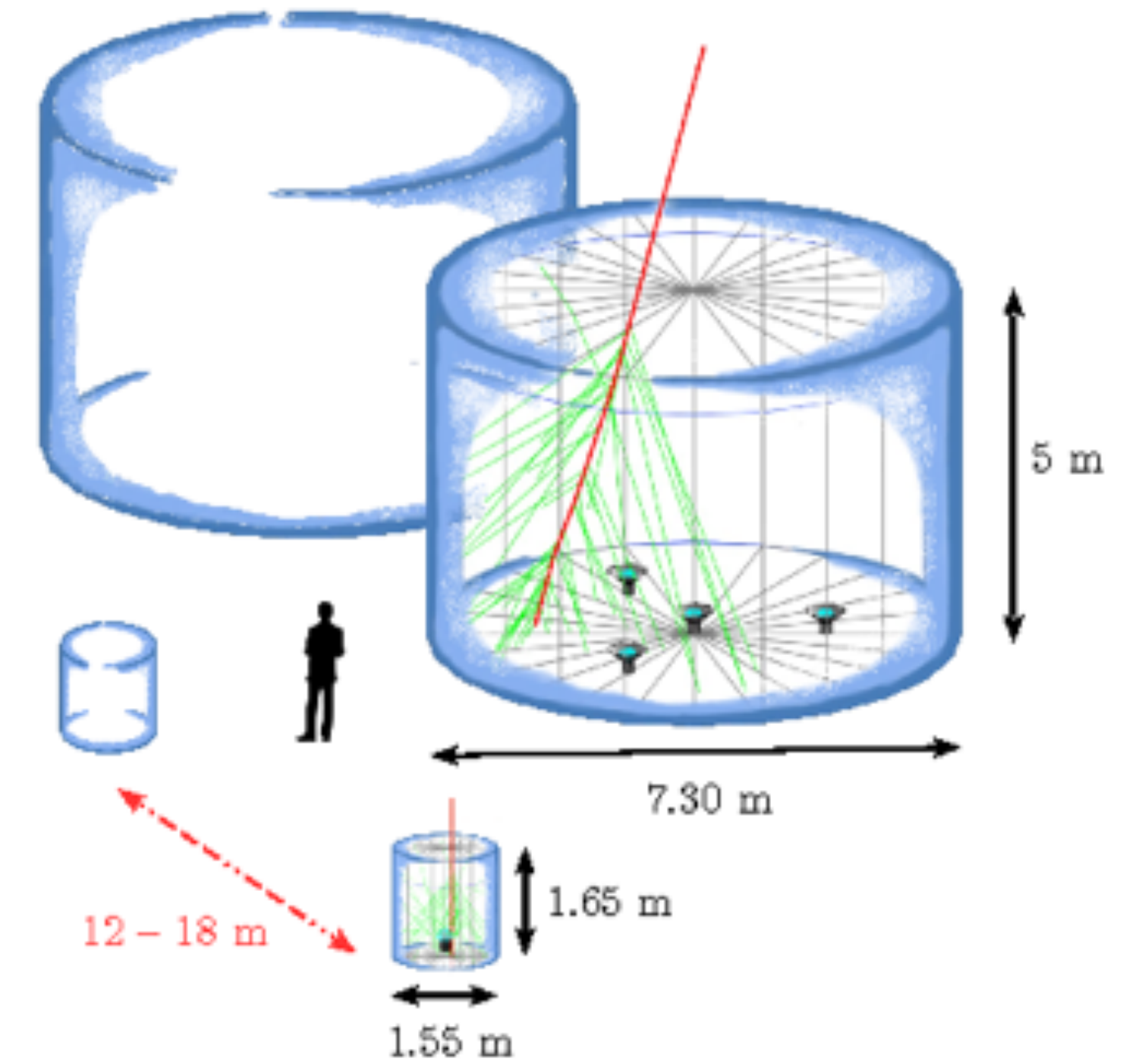
- In hadronic-only scenario protons of at least 250 TeV produce gamma in proton-proton interaction and secondary leptons produce radio and X-rays via synchrotron radiation.
- HAWC observation disfavours hadronic-only scenario, since observed gamma-ray emission requires $\sim 100\%$ (3×10^{50} erg) of the jet energy necessary for accelerating protons. In addition, protons should have to spread to a few degrees before emitting gamma rays.
- Acceleration is occurring in the jets, not in the central binary:
 1. Emission region is ~ 40 pc from central binary.
 2. Diffusion length scale is ~ 35 pc at these energies, assuming ISM.

Origin of the emission

SS 433 is an object which we expect particle acceleration: presence of jets and interaction regions make it a good candidate accelerator.

- Acceleration mechanism to produce ~ 1 PeV electrons.
- Acceleration in magnetic fields: possible up to a few hundred TeV. Above that, acceleration time exceeds cooling time for $16 \mu\text{G}$ fields.
- Acceleration in standing shocks (Fermi acceleration): can reach PeV energies, but at present no multi-wavelength evidence for large shocks in the interaction regions.
- The origin of the emission from SS 433 is however not clarified.

HAWC with Outriggers



- 345 water-Cherenkov detectors in a sparser array surrounding the main-array.
- Instrumented area increase by a factor of 4.
- Data recording started since 2018 August.
- Increase of well-reconstructed showers number above multi-TeV energies.

Summary and outlook

- Detection of multi TeV gamma-rays from SS 433/W50 regions, e1 and w1, with $> 5\sigma$ post-trial significance (combined) in 1017 days of HAWC observations.
- Parental particle spectra and acceleration mechanism unclear.
- Spectra of SS433 jet lobes with future measurements from HAWC.
- Perspective for improving analysis of VHE gammas from SS 433 and other binary candidates with outriggers.